frontiers | Frontiers in Earth Science

TYPE Original Research
PUBLISHED 31 October 2022
DOI 10.3389/feart.2022.952630

OPEN ACCESS

EDITED BY
Shailesh Kumar Singh,
National Institute of Water and Atmospheric Research (NIWA), New Zealand

REVIEWED BY
Jun Hou,
Hohai University, China
Feng Pan,
Xiamen University, China

*CORRESPONDENCE
Minghong Chen,
chenminghong@cau.edu.cn

SPECIALTY SECTION
This article was submitted to Hydrosphere, a section of the journal Frontiers in Earth Science

RECEIVED 25 May 2022
ACCEPTED 01 August 2022
PUBLISHED 31 October 2022

CITATION
Li Y, Chen M and Liu X (2022), Vertical distribution and transformation of phosphorus and iron in paddy soils during the whole growth stage of rice. *Front. Earth Sci.* 10:952630. doi: 10.3389/feart.2022.952630

Vertical distribution and transformation of phosphorus and iron in paddy soils during the whole growth stage of rice

Yun Li, Minghong Chen* and Xuanye Liu

College of Water Resources and Civil Engineering, China Agricultural University, Beijing, China

Paddy fields have alternating wet and dry hydrological cycles at different growth stages of rice, driving changes in soil environment and phosphorus (P) transformation and transport. *In-situ* measurements of dissolved oxygen (DO), iron (Fe), and P concentrations were conducted to determine the vertical distribution of these concentrations together with the hydrological and meteorological data during the whole growth stage. The results demonstrate that soil vertical DO concentrations at different growth stages were greatly influenced by the water level and temperature of the paddy field at the soil-water interface. A strong negative correlation between soil DO and DGT-labile Fe has been observed, whereas a strong positive correlation has been observed between soil Fe concentration and vertical P. In the paddy field, soil DO concentrations were lower during tillering, booting, and heading to flowering than during the other stages. Thus, soluble P fluxes from soil water interfaces (SWIs) to overlying waters were most significant during these three stages. Furthermore, soils in these three stages are capable of sustained release of P and are highly able to buffer P. Consequently, water management in paddy fields should take into account the hydrological environment during these three stages in order to minimize soil P release. The results of our study provide a valuable reference point for controlling soil P and Fe during rice growth.

KEYWORDS

paddy field, hydrological environment, vertical distribution, growth stage, soil phosphorus, phosphorus flux

1 Introduction

Rice growth mainly depends on irrigation water and soil nutrients in the field (Acosta-Motos et al., 2020; Bi et al., 2021). The farming process drains nutrients from the field, reducing soil fertility and causing paddy soils to lose nutrients (Adimassu et al., 2020; Mao et al., 2020; Alvarez et al., 2021; Huo et al., 2021). Therefore, changes in the hydrological environment of paddy fields have a significant impact on the loss of nutrients. Appropriate water management is vital to nutrient loss (Shi et al., 2018; Mao et al., 2020).

Rice requires phosphorus (P) as one of its major nutrients, with different fertility stages and different depths of the root system requiring different nutrients (Fink et al.,

2016; Crumpton et al., 2020). Changes in soil-water nutrient fluxes due to the changes of the hydrological environmental factors in paddy fields (Liptzin and Silver, 2009; Kuzyakov and Razavi, 2019; Bhadha et al., 2020). P and iron (Fe) are cyclically converted into dissolved oxygen (DO) by moisture-driven fluctuations. Several studies have pointed out that moisture conditions affect the amount of radial oxygen loss from the soil and the transformation of Fe ions (Tinh et al., 2006; Xie et al., 2020). The growth of rice is accompanied by changes in the hydrological environment of paddy fields. As rice is a flooded crop, flooding tends to reduce the amount of oxygen in the soil, which results in the reduction and dissolution of Fe present as hydroxide, while P is resolved and released into the pore water. A coupling relationship exists between the distribution of vertical iron and phosphorus concentrations in soils (Becker and Asch, 2005; Wang et al., 2018). Consequently, the research on the vertical soil concentration and the correlation of DO, P, Fe under the influence of the hydrological environment in paddy fields is essential for understanding the P uptake in rice (Wen et al., 2019).

In recent years, sediments have been receiving greater attention for their variation in P and Fe. In the past, many studies focused on the simultaneous changes of P and Fe contents in coastal and lake as well as wetland sediments (Zhang et al., 2018; Pan et al., 2019, 2020; Yang et al., 2019). Studies have shown that the redox environment of sediments and the cycling of Fe are critical for the fixation of sediment P (Zhang et al., 2018; Pan et al., 2020). Since phosphate is mainly adsorbed on iron particles, making the unstable P strongly positively correlated with Fe content (Wang et al., 2005; Li et al., 2021). P in sediment pore water in anoxic flooded areas is often a source of P to the overlying water (Pan et al., 2019). Meanwhile, the cyclic coupling of Fe and P was influenced by the vegetation root system (Xiao et al., 2022). In addition, Wang et al. (2019) was also examined the distribution of P and Fe concentrations in paddy soils under high and low P conditions.

However, the water column environment of paddy soils is more drastically changed during the year compared to sediments, and their DO, Fe and P patterns can be quite different from those of sediments (Acosta-Motos et al., 2020; Bi et al., 2021). Fertilization and irrigation of paddy fields not only changed the conditions of P concentration in the field, but also strongly varied the hydrological environment (water level, water temperature, dissolved oxygen and pH, *etc.*) (Eltohamy et al., 2021). Due to the changes in the hydrological environment of paddy fields, it would be worthwhile to study the variation patterns in DO, Fe and P in paddy soils at different growth stages. In this way, direct evidence can be provided for the discharge of P from soil to the overlying water and the irrigation scheme during the whole growth stage of the paddy field.

Rice growth is accompanied by changes in meteorological conditions and field management practices, which can have a large impact on the hydrological environment of paddy fields (Song, 2018). By combining the interaction mechanisms of DO, Fe, and P, we investigated the transport of soil P in paddy fields during the whole growth stage. We investigated the vertical distribution and correlation of DO, P and Fe concentrations in the paddy field using *in situ* measurement technique and the tillering stage as a typical fertility stage in the paddy field. Meanwhile, *in situ* measurements were conducted to study the vertical transformation of P and Fe under different growing stages and changing hydrological conditions.

2 Materials and methods

2.1 Study area and sampling sites

The experiment was conducted at the Heping Irrigation District Experimental Station in Suihua City, Heilongjiang Province, China (127°17′ ~ 127°49′ E, 46°34′ ~ 47°07′ N). One *in-situ* monitoring site was selected in a small paddy field for rice cultivation. The size of the experimental field was about 10 m × 10 m. In Table 1, specific planting periods for each fertility period are shown for the rice planted between May 18 and 10 September 2021. The water level of the paddy field is controlled at about 0–60 mm during the whole growth stage. Drainage and transplanting of rice are carried out after the ponding stage. The long tillering stage and significant hydrological environmental changes dictated the use of two *in situ* monitoring sites for parallel experiments during the tillering stage. The paddy fields were observed once during the entire growth stage (ponding stage, reviving stage, tillering stage, booting stage, heading to flowering stage, and milky ripening stage).

2.2 Sampling

The DO level distribution was measured *in situ* in the soil profile using a Unisense microelectrode device (PreSens GmbH, Regensburg, Germany). The thruster can insert the DO electrode to 30 mm below the soil in 2 mm or 5 mm steps and convert the electrical signal into concentration values based on a pre-set standard curve. As a result of the visualization process, a map of the DO concentration distribution over the soil vertical distribution is obtained.

Paddy field monitoring points were equipped with high-resolution dialysis (HR-Pepper) and diffusive gradients in thin films (Zr-oxide DGT). DGT and HR-Peeper are provided by Easysensor Ltd. (www.Easysensor.net). Following deoxygenation with nitrogen for more than 24 h, the probes were stored in an oxygen-free NaCl solution and subsequently deployed in soil. To measure both SRP and soluble Fe (II), the HR-Peeper sampled soil pore water at a vertical resolution of 10 mm. The measurement of

TABLE 1 Physicochemical characteristics of the paddy soils.

Total N (g/kg)	Total P (g/kg)	Organic %	Effective iron (g/kg)	Soil texture	Particle composition/%			
					<0.002 mm	0.002–0.02 mm	0.02–0.05 mm	>0.05 mm
1.58 ± 0.33	1.08 ± 0.37	6.20	0.80	silty loam	11.25 ± 1.83	36.70 ± 3.64	29.74 ± 4.49	22.31 ± 10.55

TABLE 2 Growth stage and fertilization of rice.

Growth stage	Ponding stage	Reviving stage	Tillering stage	Booting stage	Heading to flowering stage	Milky ripening stage
Period	5.1–5.22	5.23–6.12	6.12–7.4	7.5–7.29	7.30–8.12	8.13–9.15
Fertilization	NPK fertilizer: 200–225 kg/hm^2 Urea fertilizer: 112.5 kg/hm^2 before Ponding stage	NPK fertilizer: 52.5 kg/hm^2 when filling the first water after reviving	Combined fertilizer and drug treatment: 9–12 kg/hm^2	NPK compound fertilizer: 105–150 kg/hm^2		
Average ponding depth/cm	5.42	1.69	1.39	1.51	3.16	1.68

DGT-labile P and DGT-labile Fe in one dimension using DGT. HR-Peeper and DGT were measured close to rice roots, inserted vertically and slowly, with 2–4 cm above the soil-water interface (SWI) for 48 h and 24 h, respectively. In accordance with Xu et al. (2013) and Pan et al. (2019), after removing the DGT and peeper probes from the soil, the DGT was cleaned with deionized water and placed in polyethylene bags sealed in darkness until testing.

At the same time, pH and temperature of the field water were measured and recorded with a pH meter. Automatic water level recorders were arranged in the fields to monitor the daily water level. As shown in Table 2, water levels averaged over each growth period.

2.3 Sample analysis

P and Fe were eluted from Zr-oxide DGT binding gels using a ceramic knife at 10 mm intervals. For P analysis, 1.0 mol L^{-1} NaOH solution was used, followed by rinsing with deionized water, and 1.0 mol L^{-1} HNO_3 solution was used for Fe analysis (Xu et al., 2013). P and Fe in DGT, and SRP and soluble Fe (II) in pore water were determined on an Epoch microplate spectrophotometer (Bio-Tek Instruments, Winooski, VT) using molybdenum blue (Murphy and Riley, 1962) and phenanthroline colorimetry (Tamura et al., 1974), respectively (Xu et al., 2012).

2.4 Data analysis

The cumulative mass M (μg) of DGT-labile P can be calculated as follows:

$$M = \frac{C_e V_e}{f_e} \quad (1)$$

where C_e is the measured P concentration in the eluate; V_e is the volume of the eluate; f_e is the extraction rate (Ding et al., 2012).

Following equations were used to calculate the DGT-labile P concentration C_{DGT} (mg L^{-1}) and the DGT-labile P flux F_{DGT} (pg cm^{-2} s^{-1}):

$$F_{DGT} = \frac{M}{At} \quad (2)$$

$$C_{DGT} = \frac{M\Delta g}{DAt} \quad (3)$$

where A is the exposed area of the gel strip; t is the deployment time; Δg is the thickness of the diffusion layer (0.08 cm); D is the diffusion coefficient of P in the diffusion layer (cm^2 s^{-1}) (Wang et al., 2016).

By simplification of soil-pore water kinetic exchange as a reversible sorption-resolution process, R represents the level of solids recharge into pore water after DGT absorption (Ding et al., 2010, 2016; Xing et al., 2018):

$$R = \frac{C_{DGT}}{C_{SRP}} \quad (4)$$

where C_{DGT} and C_{SRP} are labile P as measured by DGT and SRP as measured by HR-Peeper, respectively. R ranges from 0 to 1 when R equals 1 indicating a strong reactivity.

The flux of soil P through the soil-water interface (SWI) is calculated by Eqs 5–8:

$$F = \varphi D_s \frac{\partial C}{\partial X} \quad (5)$$

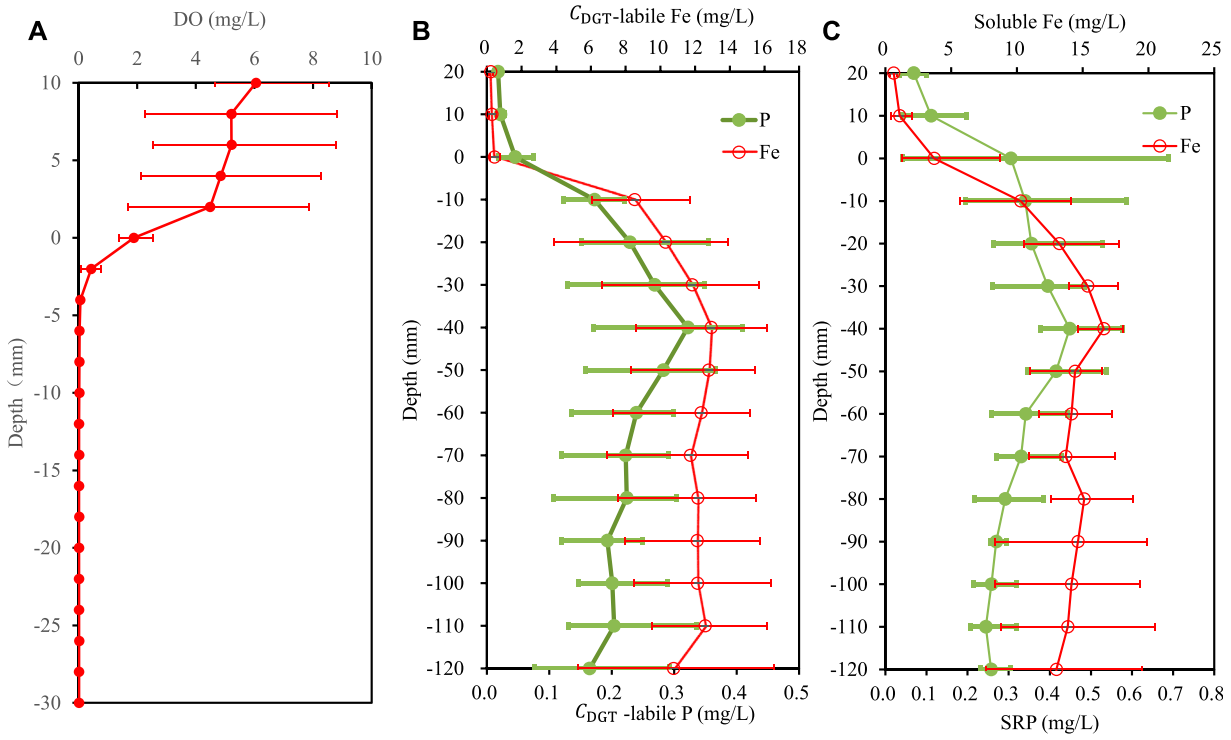

FIGURE 1
Distribution of the vertical concentrations in paddy soils. **(A)** DO concentrations, **(B)** DGT-labile P and DGT-labile Fe concentrations, and **(C)** pore water SRP and soluble Fe concentrations. Error bars indicate ± standard deviation of the mean (n =3).

$$D_s = \frac{D_0}{\varphi f} \quad (6)$$

$$f = \frac{1}{\varphi^m} \quad (7)$$

$$\varphi = \frac{(W_w - W_d)100}{W_w - W_d + \frac{W_d}{2.5}} \quad (8)$$

where φ (%) is the soil porosity. $\partial C/\partial X$ (mg L cm^{-1}) represents the concentration gradient of soil P across the SWI by calculating the sediment from 10 mm in the water covering the SWI to 10 mm below the SWI in the soil. D_s (cm^2 s^{-1}) is the soil P diffusion coefficient. D_0 (cm^2 s^{-1}) is the ideal diffusion coefficient of P. m is an empirical constant dependent on soil porosity, and m is taken as two in this study. W_w (g) and W_d (g) are the weights of wet and dry soils, respectively (Yang et al., 2019).

Data significance was determined using a one-way analysis of variance (ANOVA). It was considered statistically significant when the difference was $p < 0.01$. Linear regression was used to analyze the P and Fe relationships determined by HR-Peeper and DGT measurements. GraphPad Prism 8 was used for all statistical analyses and figures.

3 Results

3.1 Distribution and correlation of vertical DO, Fe, and P concentration in paddy soils

In the tillering stage, we illustrate the DO, Fe and P concentration distribution in soil and the correlation between the concentrations. Figure 1A shows the vertical distribution of DO in the paddy field at the tillering stage. Vertical DO concentrations in paddy soils are usually smaller and constant, and all turn at soil-water interfaces. In shallow soils, DO concentrations were higher than those in deep soils, in agreement with Bhadha et al. (2020). At the soil-water interface, DO concentrations were 1.89 mg L^{-1}, but decreased after entering the soil and tended to be 0 mg L^{-1} below 4 mm.

Figure 1B shows the vertical distributions of DGT-labile P and DGT-labile Fe concentrations in paddy soils, as well as pore water SRP and soluble Fe (II). It was observed that DGT-labile P and DGT-labile Fe concentrations increased with soil depth, but then decreased. The DGT-labile P and DGT-labile Fe concentrations in the overlying water were significantly lower than those in the paddy soil. Under aerobic conditions, Fe may form hydroxide precipitates, which promote the fixation of P (Wang et al., 2019). At about

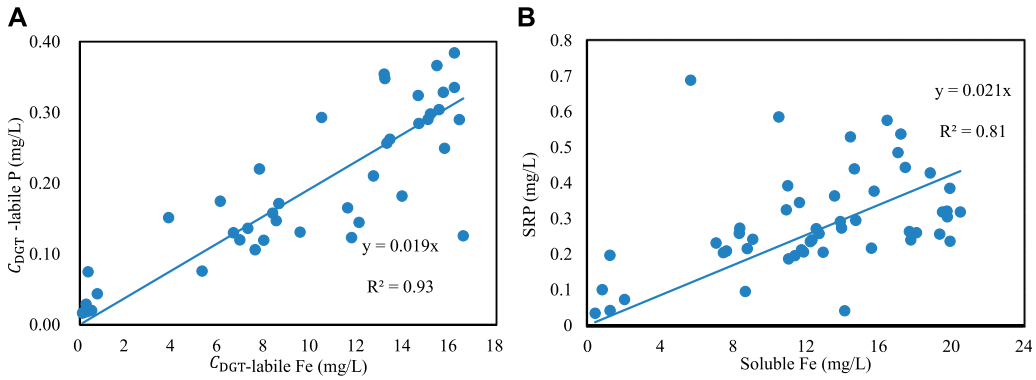

FIGURE 2
Relationships between P and Fe concentrations. **(A)** DGT-labile P and DGT-labile Fe, and **(B)** SRP and soluble Fe.

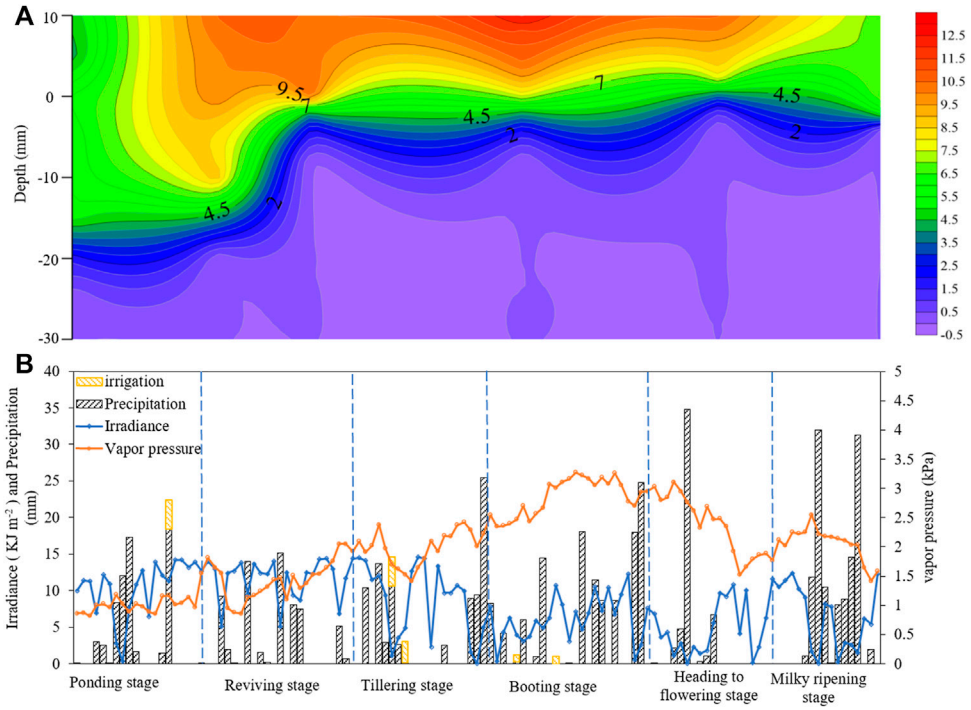

FIGURE 3
(A) Soil vertical DO concentration distribution and **(B)** meteorological factors during the whole growth stage.

40 mm of soil depth, DGT-labile P and DGT-labile Fe concentrations reached their maximum values, 0.32 mg L^{-1} and 12.93 mg L^{-1}, respectively. Figure 1C shows the vertical distributions of SRP and soluble Fe concentrations in soil pore water. Soil pore water soluble P and Fe distributions were more similar to soil DGT-labile P and DGT-labile Fe, and a significant peak was observed at 40 mm below SWI.

Figure 2 shows the correlation between vertical soil P and Fe concentrations. Several significant positive correlations were found between vertical concentrations of DGT-labile P and DGT-labile Fe, and SRP and soluble Fe concentrations in paddy soils, with Pearson correlation coefficients of $r = 0.92$ ($p<0.0001$) and $r = 0.68$ ($p<0.01$). This conclusion is consistent with the conclusions reached by several previous studies (Gao et al., 2016; Wang et al., 2019; Yang et al., 2019).

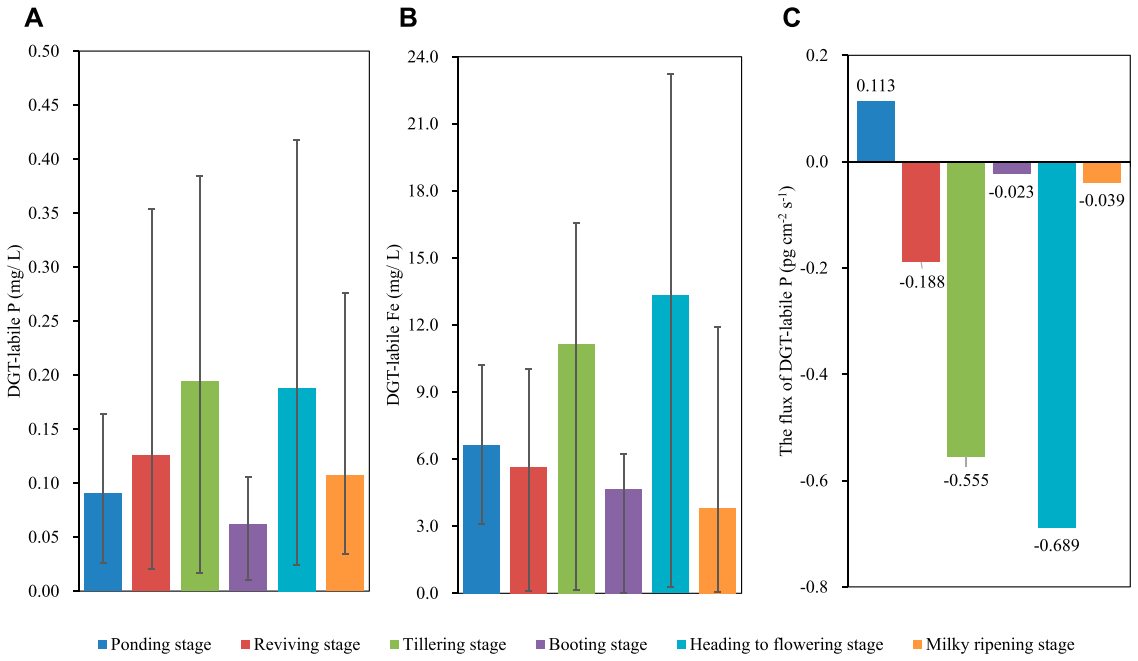

FIGURE 4
Soil vertical DGT-labile P, DGT-labile Fe during the whole growth stage of rice **(A)** Average concentration of DGT-labile P, **(B)** Average concentration of DGT-labile Fe and **(C)** DGT-labile P flux across to SWI flux.

3.2 Changes in soil vertical DO concentration distribution during the whole growth stage of paddy fields

Soil vertical DO concentrations in paddy fields during the whole growth stage of rice are shown in Figure 3A. As the depth of the paddy soil increased, the DO concentration in the overlying water decreased gradually and tended to zero. During the ponding stage, the soil depth tending to zero was the deepest of all the stages, at 25 mm below the soil surface. The reason for this might be that the soil DO concentration in the paddy field has not been depleted during the ponding stage.

An extended period of high water may affect the exchange of oxygen between paddy soil and the outside environment. During tillering, heading to flowering, and milking ripening stages, the vertical DO concentration tends to zero at soil depths near SWI with higher water levels. Based on Figure 3A, the paddy field soil had high water levels during tillering, heading to flowering, and milking ripening stages. Irrigation and precipitation are more prevalent during the tillering and heading to flowering stages, respectively. Additionally, soil DO concentration can be affected by vapor pressure in paddy fields. From the ponding stage to the booting stage, vapor pressure increased in all growth stages. According to Figure 3B, the maximum value was reached at the booting stage, then gradually decreased during the growth stage. At the soil-water interface, DO concentrations at the reviving and tillering stages were higher than at any other period of growth, measuring 9.86 and 10.51 mg L^{-1}, respectively. In addition, the fluctuations of irradiance and pH changes in the paddy soil in this study were not significant.

3.3 Changes in soil vertical DGT-labile P and DGT-labile Fe concentration distribution during the whole growth stage of paddy fields

In paddy soils at different growth stages under hydrological changes, the vertical distribution patterns and correlations of DGT-labile P and DGT-labile Fe concentrations were similar to those at the tillering stage (Data not shown).

Figures 4A,B shows the distribution of DGT-labile P and DGT-labile Fe concentrations in paddy soil by growth stage. The average concentrations of DGT-labile P and DGT-labile Fe during the whole rice growth stage reached extreme values at the same growth stage. In terms of DGT-labile P and DGT-labile Fe, the mean concentrations were higher during the tillering and heading to flowering stages, whereas the concentrations were lower during the booting stage. During heading to flowering stage, the concentration of DGT-labile P reached its highest level (13.32 mg L^{-1}). The lowest concentration of DGT-labile P was observed during milky ripening (3.80 mg L^{-1}). It was observed

TABLE 3 Pearson correlation coefficients r between vertical DO, P, and Fe concentrations in paddy soils.

	Ponding stage	Reviving stage	Tillering stage	Booting stage	Heading to flowering stage	Milky ripening stage	The whole growth stage
DGT-labile P & DGT-labile Fe	0.93****	0.71**	0.79***	0.79***	0.73**	0.92****	0.78****
SRP & Soluble Fe	0.88****	0.86****	0.85****	0.39	0.20	0.98****	0.71****
DO & DGT-labile Fe	−0.87*	−0.96***	−0.98**	−0.90*	−0.73	−0.71	0.78****
DO & Soluble Fe	−0.86**	−0.90**	−0.84	−0.28	−0.83	−0.50	0.73****

Note: ****means $p < 0.0001$, ***means $p < 0.0005$, **means $p < 0.005$, * means $p< 0.01$.

that the average concentration of DGT-labile Fe varied little over the whole growth stage, ranging from 0.06 to 0.19 mg L^{-1} for the whole growth stage.

The process of temporary releasing of P from the soil is influenced by a number of factors including the stability of the paddy soil (meteorological factors, rainfall, irrigation, *etc.*). As a less stable P component, DGT maintains P's release from paddy soils to the overlying water after the onset of hypoxia (Ding et al., 2016). As shown in Figure 4C, DGT-labile P concentrations at the soil-water interface were more stable at booting and milky ripening stages, with SWI P flux close to 0. During all growth stages except ponding, DGT-labile P fluxes were negative. The SWI of DGT-labile P was −0.555 and −0.689 pg cm^{-1} s^{-1} for tillering and heading to flowering, respectively. A possible explanation for this may be that long-term floods put the paddy soil in an anaerobic state which results in fewer resistances to the concentration-diffusion gradient process in the paddy soil. In contrast, the soil's potential to release P to the water body is enhanced (Gao et al., 2016). In the tillering and heading to flowering stages, P concentration in the overlying water needs to be monitored more closely during irrigation and drainage.

Table 3 shows the correlation between soil vertical DGT-labile P and DGT-labile Fe concentrations during rice growth. Soil vertical DGT-labile P, DGT-labile Fe, and SRP, soluble Fe concentrations were positively correlated in all growth stages of the paddy field according to Pearson correlation analysis. In particular, for DGT-labile P and DGT-labile Fe concentrations, a highly significant positive correlation ($p < 0.0001$) was observed at the ponding stage ($r = 0.93$) and the milky ripening stage ($r = 0.92$).

3.4 SRP and soluble Fe concentrations in pore water at vertical depth in paddy fields during the whole growth stage

Figures 5A,B shows the variation of average soil vertical SPR and soluble Fe concentrations at different fertility stages. Average concentrations of SRP and soluble Fe fluctuated more synchronously throughout the rice fertility period, reaching extreme values at the same time. As the growth stage progressed, the average concentrations of SRP (0.50 mg L^{-1}) and soluble Fe (19.39 mg L^{-1}) reached their maximum at the booting stage. The lowest average concentrations of SRP and soluble Fe occurred during the milky ripening stage, with 0.09 mg L^{-1} and 1.96 mg L^{-1}, respectively.

In order to better quantify the effect of the hydrological environment of the paddy field on SRP release at the soil-water interface, Figure 5C shows the flux of SRP through the SWI throughout the growth stage. Based on the results of our experiments, it was determined that the diffusion flux of SRP through the SWI ranged from −1.858 to 0.116 pg cm^{-2} s^{-1} over the entire growth period of the paddy field. In comparison to other growth stages, pore water SRP flux through the SWI was relatively low and close to zero during ponding and milky ripening. Except for reviving, SRP fluxes across SWI were negative throughout all fertility stages of rice, indicating that SRP was released from soil pore water to overlying water at all five growth stages. During the tillering stage, booting, and heading to flowering, SRP fluxes across to SWI were large negative values of −0.851, −1.858, and −1.140 pg cm^{-2} s^{-1}, respectively.

Figure 5D shows the dynamic recharge characterization parameter R for soil P during rice growth. In the paddy field, the smallest R was found during the booting stage (R = 0.13), indicating poor soil P resupply capacity. The reviving stage (R = 0.91) and the milky ripening stage (R = 0.99) showed the strongest P-responsiveness. P reactivity was moderate at the other reproductive stages, with R values between 0.60 and 0.80. Hitting the maximum R-value at the milky ripening stage indicates that the paddy soil in which the rice is planted has the most important capacity for recharging P in the soil, which is important for monitoring the P transport and transformation rate in the overlying water.

4 Discussion

In this study, the distribution of soil vertical DO concentration in paddy fields during different growth stages

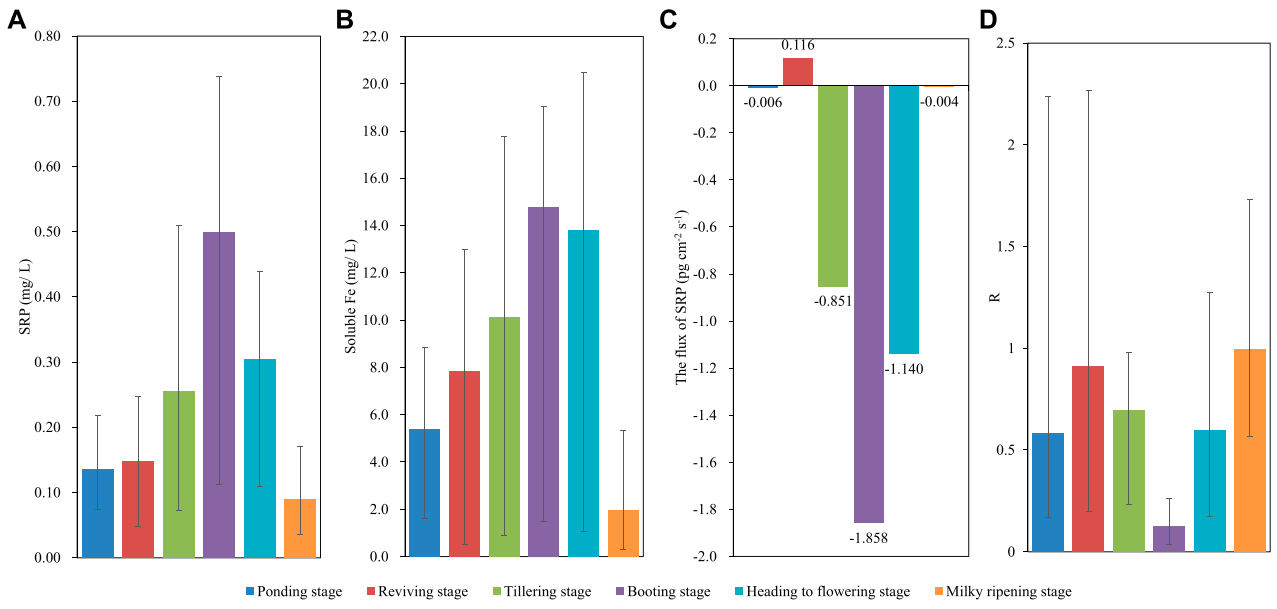

FIGURE 5
Soil vertical SRP and soluble Fe during the whole rice reproductive stage **(A)** average concentration of DGT-labile P, **(B)** average concentration of DGT-labile Fe, **(C)** SRP flux across to SWI and **(D)** the ratio R of labile P to SRP.

was investigated considering the constant changes in water level and meteorological factors in paddy fields (Zhang et al., 2018). Environmental parameters of paddy fields, such as moisture and meteorology, are essential factors influencing the diffusion of oxygen in paddy soils (Bhadha et al., 2020). In paddy fields with higher water table fertility, soil DO concentration tends to zero closer to the soil-water interface, such as during tillering and heading to flowering stages (Figure 3A). During long-term flooding of paddy fields, oxygen is rapidly discharged from the soil, resulting in a vertical stratified distribution of soil DO concentrations. The high water level of paddy soils significantly limits the transport and exchange of oxygen from the atmosphere to the soil, thus affecting the redox environment of paddy soils (Kim et al., 2021; Watanabe et al., 2021).

Changes in Fe concentration in paddy soils are controlled by soil redox conditions (Björnerås et al., 2019). Fe redox reactions are likely to occur in alternating layers with varying oxygen concentration (Uzarowicz, 2013). In paddy soils, significant negative correlations were found between DGT-labile Fe concentrations and DO concentrations, mainly at the reviving and tillering stages ($r = -0.96^{***}$ and -0.98^{**}) (Table 3). In paddy fields, the negative correlation between soil pore water Fe and DO concentration was weaker at the booting and heading to flowering stages. The reason for this may well be due to the higher level of inundation in the hydrological environment of the paddy fields during these two fertility periods, with the relationship between oxygen content and iron content being less pronounced in the upper part of the soil with low oxygen content (Ratering and Schnell, 2001).

According to Zhang et al. (2018) and Zhang et al. (2021), this study also confirmed the close relationship between P cycling in sediment/soil and Fe cycling. Throughout the whole growth stage of the paddy field, P and Fe concentrations exhibited a largely synchronous trend (Figure 2). With the exception of the stages associated with the booting and heading to flowering, vertical concentrations of DGT-labile Fe and DGT-labile P (r = 0.78) as well as pore water soluble Fe and SRP concentrations (r = 0.73) showed a strong correlation in paddy soils during the whole growth stage, especially during the ponding stage and the milky ripening stage. This shows that strong coupling between Fe and P concentrations does exist in paddy soils (Huang et al., 2016; Li et al., 2021). At higher redox potentials, ferrous iron from soil pore water is converted to insoluble Fe oxide-hydroxide precipitation, forming phosphorus-rich iron spots on the surface of rice roots (Xing et al., 2018; Marzocchi et al., 2019). The lower redox potential under the anoxic conditions formed by prolonged flooding leads to the dissolution of Fe (III) oxides, which releases P into the paddy soil (Marzocchi et al., 2019; Wei et al., 2019). Wei et al. (2019) showed that the decrease in soil redox potential during the head to flowering stage led to the collapse of iron spots in the rice root system

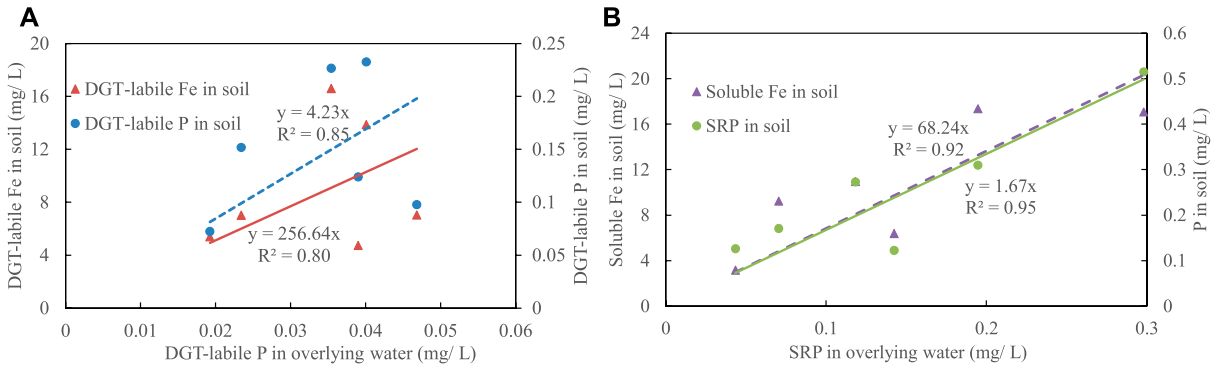

FIGURE 6
Relationships between P and Fe concentrations in soil and overlying water. **(A)** DGT-labile P and DGT-labile Fe, and **(B)** SRP and soluble Fe.

and release of P into the soil. In soil, this mechanism results in simultaneous changes in P and Fe labiles or solubles. Rice roots with iron spots form at high redox potentials, which facilitate enhanced P uptake. In this way, P is conserved in the soil, providing essential nutrients for rice growth (Yerokun, 2008; Liptzin and Silver, 2009). Changes in redox potential of paddy soils is important in the transformation of Fe and P in soils (Marschner, 2021).

Due to the P concentration difference between the paddy soil and the overlying water, a certain exchange of P concentration exists among them (Pan et al., 2020). P diffuses upward due to the concentration gradient, with iron easily forming hydroxides in the presence of oxygen, to form compounds of Fe and P (Pan et al., 2019). Therefore, the P and Fe concentrations above the SWI interface were smaller compared to the vertical concentration of P and Fe in paddy soils. This is especially important for the tillering and heading to flowering stages where soil P concentration is high. In order to better clarify the relationship between the hydrological environment of paddy fields on vertical DO, P, and Fe concentrations, we analyzed the relationship between the P concentration in the overlying water of paddy fields and the vertical P and Fe concentrations in the soil. Large concentrations of P were present in the overlying water of the paddy field during the booting stage (0.30 mg L^{-1}) and the head to flowering stage (0.19 mg L^{-1}). Meanwhile, strong linear correlations were found between the DGT-labile and pore water P concentrations in the overlying water of the paddy field and both vertical P and Fe concentrations in the soil (Figures 6A,B). Overlying water P concentrations were correlated with vertical soil P ($p < 0.1$) and Fe ($p < 0.1$). To maintain the appropriate water quality of paddy fields during the booting and heading to flowering stages, a low water layer should be maintained.

During the entire growth stage of the paddy field, changes in water level and meteorological conditions caused cyclical variations in DO concentrations. DO in paddy soils controls rice phosphorus uptake directly or indirectly through ferrous ions (Frenzel et al., 1999; Li and Wang, 2013; Mei et al., 2014). During tillering, booting, and heading to flowering stages, the depth of DO concentration in the soil increasing to 0 was close to the soil-water interface (>10 mm below the surface of the soil). It is important to note that all three of these growth stages released significant fluxes of SRP across from SWI to the overlying water at the same time. Consequently, rice crop irrigation methods must be controlled, such as reducing irrigation during the tillering stage and relying on controlled irrigation, shallow Sun irrigation, and shallow wet irrigation. During the booting and head-to-flowering stage when P concentration is high, the diffusion of vertical DO concentration in paddy soils is regulated by water level or soil water content.

5 Conclusion

We conducted *in situ* experiments in the field to determine the vertical distribution of DO, Fe, and P concentrations in soil at different growth stages. A strong correlation was found between vertical DO, P, and Fe concentrations in paddy soils. Changes in the hydrological environment at different growth stages affected the soil vertical DO concentrations, leading to corresponding changes in soil vertical P and Fe concentrations. During the tillering, booting, and heading to flowering stages, special attention should be paid to the quantity of irrigation water and the hydrological environment. According to the results, water management in paddy fields may influence soil Fe and P movement through redox conditions (such as DO concentrations). Consequently, proper paddy water management can reduce soil P loss and environmental pollution.

Data availability statement

The original contributions presented in the study are included in the article/Supplementary Material, further inquiries can be directed to the corresponding author.

Author contributions

YL: Writing-original draft, Formal analysis, Data Curation, Visualization. MC: Writing-original draft, Writing-Review & Editing, Investigation, Funding acquisition. XL: Writing-Review & Editing, Investigation, Methodology.

Funding

This work was supported by the National Natural Science Foundation of China (Grant No. 52079137) and the National Key Research and Development Program of the Chinese Ministry of Science and Technology (Grant No. 2016YFC0400107).

Conflict of interest

The authors declare that the research was conducted in the absence of any commercial or financial relationships that could be construed as a potential conflict of interest.

Publisher's note

All claims expressed in this article are solely those of the authors and do not necessarily represent those of their affiliated organizations, or those of the publisher, the editors and the reviewers. Any product that may be evaluated in this article, or claim that may be made by its manufacturer, is not guaranteed or endorsed by the publisher.

Supplementary material

The Supplementary Material for this article can be found online at: https://www.frontiersin.org/articles/10.3389/feart.2022.952630/full#supplementary-material

References

Acosta-Motos, J. R., Rothwell, S. A., Massam, M. J., Albacete, A., Zhang, H., and Dodd, I. C. (2020). Alternate wetting and drying irrigation increases water and phosphorus use efficiency independent of substrate phosphorus status of vegetative rice plants. *Plant Physiology Biochem.* 155, 914–926. doi:10.1016/j.plaphy.2020.06.017

Adimassu, Z., Tamene, L., and Degefie, D. T. (2020). The influence of grazing and cultivation on runoff, soil erosion, and soil nutrient export in the central highlands of Ethiopia. *Ecol. Process.* 9, 23. doi:10.1186/s13717-020-00230-z

Alvarez, A. L., Weyers, S. L., Johnson, J. M. F., and Gardner, R. D. (2021). Soil inoculations with Anabaena cylindrica improve aggregate stability and nutrient dynamics in an arable soil and exhibit potential for erosion control. *J. Appl. Phycol.* 33, 3041–3057. doi:10.1007/s10811-021-02526-9

Bhadha, J. H., Khatiwada, R., Tootoonchi, M., and Capasso, J. (2020). Interpreting redox potential (Eh) and diffusive fluxes of phosphorus (P) and nitrate (NO3−) from commercial rice grown on histosols. *Paddy Water Environ.* 18, 167–177. doi:10.1007/s10333-019-00772-9

Becker, M., and Asch, F. (2005). Iron toxicity in rice—Conditions and management concepts. *Z. Pflanzenernähr. Bodenk.* 168, 558–573. doi:10.1002/jpln.200520504

Bi, J., Hou, D., Zhang, X., Tan, J., Bi, Q., Zhang, K., et al. (2021). A novel water-saving and drought-resistance rice variety promotes phosphorus absorption through root secreting organic acid compounds to stabilize yield under water-saving condition. *J. Clean. Prod.* 315, 127992. doi:10.1016/j.jclepro.2021.127992

Björnerås, C., Škerlep, M., Floudas, D., Persson, P., and Kritzberg, E. S. (2019). High sulfate concentration enhances iron mobilization from organic soil to water. *Biogeochemistry* 144, 245–259. doi:10.1007/s10533-019-00581-6

Crumpton, W. G., Stenback, G. A., Fisher, S. W., Stenback, J. Z., and Green, D. (2020). Water quality performance of wetlands receiving non, oint source nitrogen loads: Nitrate and total nitrogen removal efficiency and controlling factors. *J. Environ. Qual* 49, 735–744. doi:10.1002/jeq2.20061

Ding, S., Sun, Q., Xu, D., Jia, F., He, X., and Zhang, C. (2012). High-resolution simultaneous measurements of dissolved reactive phosphorus and dissolved sulfide: The first observation of their simultaneous release in sediments. *Environ. Sci. Technol.* 46, 8297–8304. doi:10.1021/es301134h

Ding, S., Wang, Y., Wang, D., Li, Y. Y., Gong, M., and Zhang, C. (2016). *In situ*, high-resolution evidence for iron-coupled mobilization of phosphorus in sediments. *Sci. Rep.* 6, 24341. doi:10.1038/srep24341

Ding, S., Xu, D., Sun, Q., Yin, H., and Zhang, C. (2010). Measurement of dissolved reactive phosphorus using the diffusive gradients in thin films technique with a high-capacity binding phase. *Environ. Sci. Technol.* 44, 8169–8174. doi:10.1021/es1020873

Eltohamy, K. M., Liu, C., Khan, S., Niyungeko, C., Jin, Y., Hosseini, S. H., et al. (2021). An internet-based smart irrigation approach for limiting phosphorus release from organic fertilizer-amended paddy soil. *J. Clean. Prod.* 293, 126254. doi:10.1016/j.jclepro.2021.126254

Fink, J. R., Inda, A. V., Tiecher, T., and Barrón, V. (2016). Iron oxides and organic matter on soil phosphorus availability. *Ciênc. Agrotec.* 40, 369–379. doi:10.1590/1413-70542016404023016

Frenzel, P., Bosse, U., and Janssen, P. H. (1999). Rice roots and methanogenesis in a paddy soil: Ferric iron as an alternative electron acceptor in the rooted soil. *Soil Biol. Biochem.* 31, 421–430. doi:10.1016/s0038-0717(98)00144-8

Gao, Y., Liang, T., Tian, S., Wang, L., Holm, P. E., and Hansen, H. C. B. (2016). High-resolution imaging of labile phosphorus and its relationship with iron redox state in lake sediments. *Environ. Pollut.* 219, 466–474. doi:10.1016/j.envpol.2016.05.053

Huang, S., Chen, C., Peng, X., and Jaffé, P. R. (2016). Environmental factors affecting the presence of Acidimicrobiaceae and ammonium removal under iron-reducing conditions in soil environments. *Soil Biol. Biochem.* 98, 148–158. doi:10.1016/j.soilbio.2016.04.012

Huo, J., Liu, C., Yu, X., Chen, L., Zheng, W., Yang, Y., et al. (2021). Direct and indirect effects of rainfall and vegetation coverage on runoff, soil loss, and nutrient loss in a semi-humid climate. *Hydrol. Process.* 35, 13985. doi:10.1002/hyp.13985

Kim, S., Kim, H.-B., Kwon, E. E., and Baek, K. (2021). Mitigating translocation of arsenic from rice field to soil pore solution by manipulating the redox conditions. *Sci. Total Environ.* 762, 143124. doi:10.1016/j.scitotenv.2020.143124

Kuzyakov, Y., and Razavi, B. S. (2019). Rhizosphere size and shape: Temporal dynamics and spatial stationarity. *Soil Biol. Biochem.* 135, 343–360. doi:10.1016/j.soilbio.2019.05.011

Li, R., Gao, L., Wu, Q., Liang, Z., Hou, L., Yang, Z., et al. (2021a). Release characteristics and mechanisms of sediment phosphorus in contaminated and uncontaminated rivers: A case study in south China. *Environ. Pollut.* 268, 115749. doi:10.1016/j.envpol.2020.115749

Li, Y., Shahbaz, M., Zhu, Z., Deng, Y., Tong, Y., Chen, L., et al. (2021b). Oxygen availability determines key regulators in soil organic carbon mineralisation in paddy soils. *Soil Biol. Biochem.* 153, 108106. doi:10.1016/j.soilbio.2020.108106

Li, Y., and Wang, X. (2013). Root-induced changes in radial oxygen loss, rhizosphere oxygen profile, and nitrification of two rice cultivars in Chinese red soil regions. *Plant Soil* 365, 115–126. doi:10.1007/s11104-012-1378-1

Liptzin, D., and Silver, W. L. (2009). Effects of carbon additions on iron reduction and phosphorus availability in a humid tropical forest soil. *Soil Biol. Biochem*. 41, 1696–1702. doi:10.1016/j.soilbio.2009.05.013

Mao, Y.-T., Hu, W., Chau, H. W., Lei, B.-K., Di, H.-J., Chen, A.-Q., et al. (2020). Combined cultivation pattern reduces soil erosion and nutrient loss from sloping farmland on red soil in southwestern China. *Agronomy* 10, 1071. doi:10.3390/agronomy10081071

Marschner, P. (2021). Processes in submerged soils – linking redox potential, soil organic matter turnover and plants to nutrient cycling. *Plant Soil* 464, 1–12. doi:10.1007/s11104-021-05040-6

Marzocchi, U., Benelli, S., Larsen, M., Bartoli, M., and Glud, R. N. (2019). Spatial heterogeneity and short-term oxygen dynamics in the rhizosphere of Vallisneria spiralis : Implications for nutrient cycling. *Freshw. Biol*. 64, 532–543. doi:10.1111/fwb.13240

Murphy, J., and Riley, J. P. (1962). A modified single solution method for the determination of phosphate in natural waters. *Anal. Chim. Acta*. 27, 31–36. doi:10.1016/S0003-2670(00)88444-5

Mei, X.-Q., Yang, Y., Tam, N. F.-Y., Wang, Y.-W., and Li, L. (2014). Roles of root porosity, radial oxygen loss, Fe plaque formation on nutrient removal and tolerance of wetland plants to domestic wastewater. *Water Res*. 50, 147–159. doi:10.1016/j.watres.2013.12.004

Pan, F., Guo, Z., Cai, Y., Fu, Y., Wu, J., Wang, B., et al. (2020). Cyclical patterns and (im)mobilization mechanisms of phosphorus in sediments from a small creek estuary: Evidence from *in situ* monthly sampling and indoor experiments. *Water Res*. 171, 115479. doi:10.1016/j.watres.2020.115479

Pan, F., Liu, H., Guo, Z., Li, Z., Wang, B., Cai, Y., et al. (2019). Effects of tide and season changes on the iron-sulfur-phosphorus biogeochemistry in sediment porewater of a mangrove coast. *J. Hydrology* 568, 686–702. doi:10.1016/j.jhydrol.2018.11.002

Ratering, S., and Schnell, S. (2001). Nitrate-dependent iron(II) oxidation in paddy soil. *Environ. Microbiol*. 3, 100–109. doi:10.1046/j.1462-2920.2001.00163.x

Shi, W., Huang, M., and Wu, L. (2018). Prediction of storm-based nutrient loss incorporating the estimated runoff and soil loss at a slope scale on the Loess Plateau. *Land Degrad. Dev*. 29, 2899–2910. doi:10.1002/ldr.3028

Song, T., Xu, F., Yuan, W., Zhang, Y., Liu, T., Chen, M., et al. (2018). Comparison on physiological adaptation and phosphorus use efficiency of upland rice and lowland rice under alternate wetting and drying irrigation. *Plant Growth Regul*. 16, 195–210. doi:10.1007/s10725-018-0421-5

Tamura, H., Goto, K., Yotsuyanagi, T., and Nagayama, M. (1974). Spectrophotometric determination of iron(II) with 1,10-phenanthroline in the presence of large amounts of iron(III). *Talanta*. 21, 314–318. doi:10.1016/0039-9140(74)80012-3

Tinh, T. K., Huong, H. T. T., and Nilsson, S. I. (2006). Rice-soil interactions in Vietnamese acid sulphate soils: Impacts of submergence depth on soil solution chemistry and yields. *Soil Use Manag*. 17, 67–76. doi:10.1111/j.1475-2743.2001.tb00011.x

Uzarowicz, Ł. (2013). Microscopic and microchemical study of iron sulphide weathering in a chronosequence of technogenic and natural soils. *Geoderma* 198, 137–150. doi:10.1016/j.geoderma.2013.01.006

Wang, S., Jin, X., Pang, Y., Zhao, H., Zhou, X., and Wu, F. (2005). Phosphorus fractions and phosphate sorption characteristics in relation to the sediment compositions of shallow lakes in the middle and lower reaches of Yangtze River region, China. *J. colloid interface Sci*. 289, 339–346. doi:10.1016/j.jcis.2005.03.081

Wang, X., Lang, L., Hua, T., Li, H., Zhang, C., and Ma, W. (2018). Effects of aeolian processes on soil nutrient loss in the gonghe basin, qinghai–tibet plateau: An experimental study. *J. Soils Sediments* 18, 229–238. doi:10.1007/s11368-017-1734-0

Wang, Y., Ding, S., Gong, M., Xu, S., Xu, W., and Zhang, C. (2016). Diffusion characteristics of agarose hydrogel used in diffusive gradients in thin films for measurements of cations and anions. *Anal. Chim. Acta* 945, 47–56. doi:10.1016/j.aca.2016.10.003

Wang, Y., Yuan, J. H., Chen, H., Zhao, X., Wang, D., Wang, S. Q., et al. (2019). Small-scale interaction of iron and phosphorus in flooded soils with rice growth. *Sci. Total Environ*. 669, 911–919. doi:10.1016/j.scitotenv.2019.03.054

Watanabe, T., Katayanagi, N., Agbisit, R., Llorca, L., Hosen, Y., and Asakawa, S. (2021). Influence of alternate wetting and drying water-saving irrigation practice on the dynamics of Gallionella-related iron-oxidizing bacterial community in paddy field soil. *Soil Biol. Biochem*. 152, 108064. doi:10.1016/j.soilbio.2020.108064

Wei, X., Zhu, Z., Wei, L., Wu, J., and Ge, T. (2019). Biogeochemical cycles of key elements in the paddy-rice rhizosphere: Microbial mechanisms and coupling processes. *Rhizosphere* 10, 100145. doi:10.1016/j.rhisph.2019.100145

Wen, Y., Zang, H., Ma, Q., Evans, C. D., Chadwick, D. R., and Jones, D. L. (2019). Is the 'enzyme latch' or 'iron gate' the key to protecting soil organic carbon in peatlands? *Geoderma* 349, 107–113. doi:10.1016/j.geoderma.2019.04.023

Xiao, K., Pan, F., Santos, I. R., Zheng, Y., Zheng, C., Chen, N., et al. (2022). Crab bioturbation drives coupled iron-phosphate-sulfide cycling in mangrove and salt marsh soils. *Geoderma* 424, 115990. doi:10.1016/j.geoderma.2022.115990

Xie, Y., Fang, Q., Li, M., Wang, S., Luo, Y., Wu, X., et al. (2020). Low concentration of Fe(II) to enhance the precipitation of U(VI) under neutral oxygen-rich conditions. *Sci. Total Environ*. 711, 134827. doi:10.1016/j.scitotenv.2019.134827

Xing, X., Ding, S., Liu, L., Chen, M., Yan, W., Zhao, L., et al. (2018). Direct evidence for the enhanced acquisition of phosphorus in the rhizosphere of aquatic plants: A case study on vallisneria natans. *Sci. Total Environ*. 616, 386–396. doi:10.1016/j.scitotenv.2017.10.304

Xu, D., Chen, Y., Ding, S., Sun, Q., Wang, Y., and Zhang, C. (2013). Diffusive gradients in thin films technique equipped with a mixed binding gel for simultaneous measurements of dissolved reactive phosphorus and dissolved iron. *Environ. Sci. Technol*. ,47, 10477–10484. doi:10.1021/es401822x

Xu, D., Wu, W., Ding, S., Sun, Q., and Zhang, C. (2012). A high-resolution dialysis technique for rapid determination of dissolved reactive phosphate and ferrous iron in pore water of sediments. *Sci. Total Environ*. 421–422, 245–252. doi:10.1016/j.scitotenv.2012.01.062

Yang, C., Tong, L., Liu, X., Tan, Q., and Liu, H. (2019). High-resolution imaging of phosphorus mobilization and iron redox cycling in sediments from Honghu Lake, China. *J. Soils Sediments* 19, 3856–3865. doi:10.1007/s11368-019-02342-2

Yerokun, O. A. (2008). Chemical characteristics of phosphorus in some representative benchmark soils of Zambia. *Geoderma* 147, 63–68. doi:10.1016/j.geoderma.2008.07.007

Zhang, L., Tang, Z., Zhang, S., Jia, X., Yu, X., Sun, G., et al. (2018). Effects of artificial aeration and iron inputs on the transformation of carbon and phosphorus in a typical wetland soil. *J. Soils Sediments* 18, 3244–3255. doi:10.1007/s11368-018-1988-1

Zhang, Y., Li, C., Sun, Q., Jiang, C., Ding, S., Chen, M., et al. (2021). Phosphorus acquisition strategy of Vallisneria natans in sediment based on *in situ* imaging techniques. *Environ. Res*. 202, 111635. doi:10.1016/j.envres.2021.111635